Journal of Rock Mechanics and Geotechnical Engineering 16 (2024) 1398–1410

Contents lists available at ScienceDirect

Journal of Rock Mechanics and Geotechnical Engineering

journal homepage: www.jrmge.cn

Full Length Article

Stabilisation of estuarine sediments with an alkali-activated cement for deep soil mixing applications

Claver Pinheiro [a], Sara Rios [b,*], António Viana da Fonseca [b], Nuno Cristelo [c]

[a] Centre of Physics of Minho and Porto Universities (CF-UM-UP), Azurém Campus, University of Minho, Guimarães, 4800-058, Portugal
[b] CONSTRUCT-GEO, Faculty of Engineering, University of Porto, Rua Dr. Roberto Frias, Porto, s/n 4200-465, Portugal
[c] CQ-VR, School of Science and Technology, University of Trás-os-Montes e Alto Douro, Vila Real, 5000-801, Portugal

ARTICLE INFO

Article history:
Received 23 January 2023
Received in revised form
20 June 2023
Accepted 14 August 2023
Available online 4 December 2023

Keywords:
Alkaline-activation
Steel slag
Submerged curing
Seismic wave measurements
Leachate analysis
Curing under stress

ABSTRACT

In this work, an alternative alkali-activated cement (AAC) made of ladle slag precursor mixed with sodium hydroxide and sodium silicate has been developed to enhance the bearing capacity of estuarine soils in coastal conditions via deep soil mixing (DSM). The AAC was optimized to use a low reactivity precursor (ladle slag) and to deal with a contaminated high-water content natural sediment cured under water. The material performance was analysed by comparison to a mixture made with Portland cement and cured in the same conditions. Flexural and unconfined compressive strength tests as well as seismic waves measurements after 3-, 7-, 14- and 28-d curing were performed to obtain a relationship between elastic stiffness and strength with curing time for both mixtures. Remarkably, the AAC mix demonstrated superior strength results, exhibiting almost double flexural and compressive strengths after 28 d compared to the Portland cement mix. The AAC mix also showed a higher rate of stiffness increase than the Portland cement mix, which has a higher initial stiffness at young ages but lower stiffness evolution. Leachate analysis confirmed that the proposed AAC could effectively immobilise any contaminants from soil or precursors. The effect of curing under stress was analysed in triaxial compression tests and found to be insignificant, indicating that laboratory data obtained without stress curing can represent the material's behaviour in a DSM column, which will cure under the weight of the column.

1. Introduction

Deep soil mixing (DSM) is a very versatile ground improvement solution, applied with different objectives, such as the reduction of embankment settlements (Venda Oliveira et al., 2011; Gupta and Kumar, 2023), slope stabilisation (Jamsawang et al., 2015; Zuo et al., 2023), liquefaction mitigation (Nguyen et al., 2013; Hasheminezhad and Bahadori, 2019), retaining structures (Shao et al., 2005; Cortes-Garcia and Chartier, 2022), solidification of estuarine sediments (Maher et al., 2007; Bouassida et al., 2022), or remediation of contaminated sites with low permeability containment walls (Wang et al., 2015; Freitag et al., 2021).

The DSM technique is typically applied using Portland cement as the binder. To help mitigate the environmental concerns related with the production of Portland cement, i.e. the release of carbon dioxide to the atmosphere and the extraction of natural raw materials (Turner and Collins, 2013; Mohammed et al., 2021), a new type of binder, based on industrial by-products, was studied in the present work. The alkaline activation of fly ash or slags creates an alkali-activated cement (AAC) capable of replacing Portland cement in many situations (Provis and van Deventer, 2014; Grant Norton and Provis, 2020). For instance, it has proved to be very effective in immobilising heavy metals present in some industrial wastes and residues used as precursors. Some of those residues are fly ash from coal-fired power plants (Phair et al., 2004) or from municipal solid waste incineration (Gao et al., 2017). AAC has also been used for the stabilisation of hazardous and radioactive wastes (Rakhimova, 2022; Tyagi and Annachhatre, 2023). In some cases, AAC are cured under high temperatures (>30 °C) which significantly increases the reaction rate and resulting strength values (Talha Junaid et al., 2017). However, its application in soil stabilisation (including DSM), even at low curing temperatures, has been demonstrated by several researchers (Sargent et al., 2016; Arulrajah et al., 2018; Mohammadinia et al., 2019).

* Corresponding author.
E-mail address: sara.rios@fe.up.pt (S. Rios).
Peer review under responsibility of Institute of Rock and Soil Mechanics, Chinese Academy of Sciences.

https://doi.org/10.1016/j.jrmge.2023.08.020

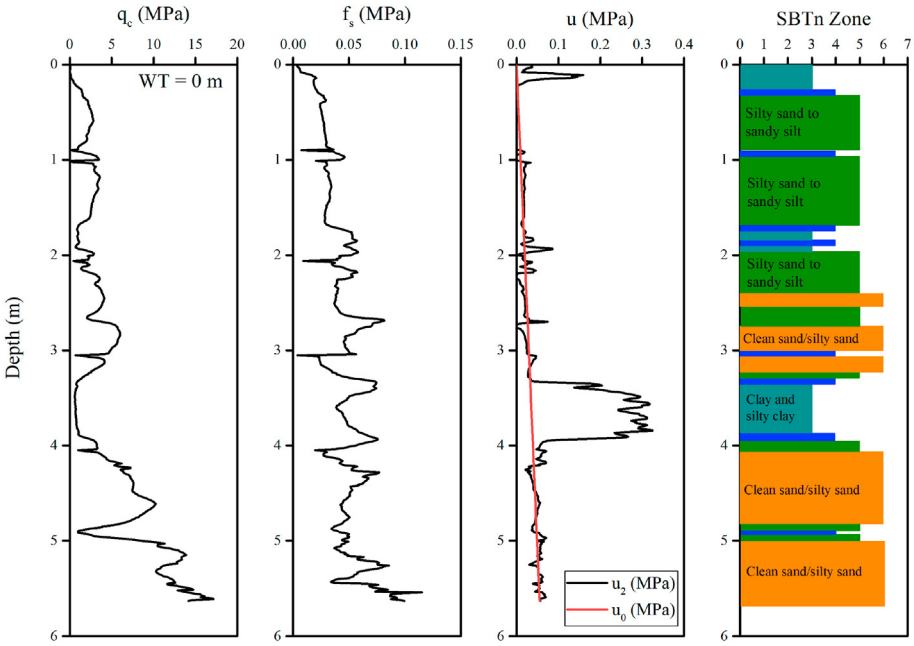

Fig. 1. CPTU profile for the second point including the cone resistance (q_c), the sleeve friction (f_s) and the pore pressure (u) measured in the test as well as the normalized soil behaviour type classification (SBTn).

Sargent et al. (2016) simulated the dry DSM using sodium hydroxide pellets to activate a ground granulated blast furnace slag (GGFS) for the stabilisation of an alluvium obtaining 2 MPa of unconfined compression strength (UCS) at 28 d for the optimised mixture, which is 20 times the untreated soil strength. Their sustainability assessment also concluded that the mixture can effectively replace Portland cement with smaller carbon footprint and lower financial costs. Arulrajah et al. (2018) used an AAC made by slag, fly ash, sodium hydroxide and sodium silicate to stabilise a soft clay. For binder contents of 20% and 30%, the clay treated with AAC showed higher strength than the clay treated with cement and/or lime irrespectively of the clay moisture content. Mohammadinia et al. (2019) has used a similar binder to stabilise a fine sand concluding that high precursor contents exhibited optimum strength close to the optimum water content of the sand, whereas lower precursor contents were found to show better mechanical strength on the dry side of the optimum water content of the sand.

Conversely to previous works, the aim of the present work was to use an AAC to stabilise an acid submerged soil in a DSM column to be performed in a contaminated estuarine/coastal area in the north of Portugal. This work pretends to analyse the effect of the additional challenges that this situation brings, i.e. submerged curing and curing under stress. As observed in other estuarine soils (e.g. Kitazume et al., 2015) the pH of this soil is acid. The acid nature of the soil, the submerged curing, and the mild temperature of the curing environment were all major constraints, neither of which favouring the development of the alkaline activation reactions which are essential to produce the AAC. To better simulate field conditions, the specimens were fabricated using the high-water content of the natural sediment deposit, which is far from the value that would have been ideal in terms of binder efficiency. After the optimisation of the binder composition, the stabilised soil was tested after 3-, 7-, 14- and 28-d curing, for flexural and unconfined compression strength, while seismic wave velocity measurements were also performed, allowing the assessment of the elastic stiffness evolution with time. Leaching tests were also carried out and the resulting data were compared with the European environmental legislation, the Council Decision (LER 1701, 2004). In addition, triaxial compression tests were performed to evaluate the influence of curing under stress, which is an important issue in DSM as the material that remains at the bottom will cure under the effect of the pressures caused by the weight of the column.

Considering the important need to mitigate the Portland cement consumption, and to increase the recycling rate of available industrial by-products, this work pretended to push forward the application of the alkaline activation technique to less favourable conditions. The aim is to demonstrate that even with less reactive precursors and harsh curing conditions, alkali-activated industrial wastes can still have technically acceptable performances.

2. Site characterisation

The soil was collected near the coastal city of Vila do Conde, in northern Portugal, on the right bank of the Ave River and, specifically, near the mouth, meaning it is very exposed to the influence of tides (very wide in this region of the Atlantic coast). The soil profile was assessed by several cone penetration tests (CPTU), as reported in Rios et al. (2018). Fig. 1 presents the three measured parameters (q_c, f_s and u) obtained in the CPTU test performed at the point where the soil was collected for this study. This point is the closest to the water in the bay and for that reason the water table is at the surface. Fig. 1 also shows the normalized soil behaviour type (SBTn) classification interpretation, according to the *unified approach* proposed by Robertson (2009), which identified sands with fines, silts and a deeper layer of clay.

The in situ void ratio (e) was estimated at 0.8, based on the unit weight value of 18.6 kN/m^3 estimated from the CPTu data (Pinheiro et al., 2021). Then, the water content was estimated to be 30.55%, assuming a saturation degree of 100% (since the soil is below the water table).

A sample from the superficial silty sand layers, collected by an auger, was used throughout the present work. The soil was classified, according to the Unified Classification System (ASTM D2487-11, 2011), as sandy silt (ML), validating the CPTu classification,

and its main geotechnical properties are presented in Table 1. The soil was considered non-plastic (NP) as the Atterberg limits could not be determined, which seems reasonable as the fine fraction is mainly silt.

The chemical composition of the soil was also analysed by X-ray fluorescence, and the results are presented in Table 2. The analysis showed very similar results to those obtained by Santos-Ferreira et al. (2015) on that site, who reported sediments with a high degree of contamination, i.e. with chromium and zinc. This area was a relevant harbour facility since the middle age, used as a shipyard, where several sail boats for the XVth century Portuguese fleet were constructed, which explains the observed contamination.

The soil's mineralogical composition was characterized by X-ray diffraction (Fig. 2) which identified quartz and muscovite.

3. Materials and methods

3.1. Materials

The precursor for alkaline activation was a ladle steel slag collected at the MEGASA Steel Industry of Maia, Portugal, with no market value until the present moment. This slag is not commonly used as a precursor in alkaline activation due to its low amorphization degree (Pinheiro et al., 2020), especially when compared with that of blast furnace slag, or even coal fly ash (Adesanya et al., 2017). To overcome this deficiency, the slag was milled to increase its reactivity (Provis, 2018; Pinheiro et al., 2020). The particle size distribution (PSD) for the slag before and after milling is presented in Fig. 3, together with that of the soil. The original PSD of the slag shows a granular material slightly finer than the soil (a sandy silt), indicating that this slag is a fine material. Nevertheless, the reactivity of the slag was highly increased after the milling, as observed in preliminary tests. The chemical properties of the slag obtained by X-ray fluorescence are described in Table 3, while Fig. 4 presents its X-ray diffraction diffractogram. From Table 3, a high calcium content is observed (24%).

Sukmak et al. (2015) has shown that a high calcium fly ash can effectively stabilise a saline silty clay in an aggressive environment, while Sargent et al. (2016) successfully used GGFS to stabilise an alluvium with high-water content. This indicates that a high calcium precursor is suitable to high-water content soils in aggressive environments. For this reason, the mixtures were performed only with the ladle slag as precursor, which is an advantage in terms of cost and mixing procedures, compared with mixtures with more than one precursor, as only one material needs to be transported, stored, and mixed.

The alkaline activator was a combination of sodium hydroxide (SH) and sodium silicate (SS), both in solution form. The sodium hydroxide was purchased in flakes, with a specific gravity of 2.13 at 20 °C and 95%–99% purity. The sodium silicate was purchased already in solution form, with a specific gravity of 1.5 and a SiO_2/Na_2O ratio of 2 by mass.

Table 1
Geotechnical properties of the soil.

Property	Value
Plastic limit (ISO 17892-12, 2018)	NP
Liquid limit (ISO 17892-12, 2018)	NP
D_{50} (ISO 17892-4, 2016)	0.07 mm
Specific gravity (ISO 17892-3, 2015)	2.61
Fines fraction (ISO 17892-4, 2016)	50.52%
Uniformity coefficient (ISO 14688-2, 2017)	10.02
Curvature coefficient (ISO 14688-2, 2017)	2.72

Table 2
X-ray fluorescence soil composition.

Soil composition	Value (wt%)
Y_2O_3	0.0015
Ga_2O_3	0.002
Nb_2O_5	0.002
PbO	0.005
SrO	0.0127
Rb_2O	0.0241
MnO	0.0282
ZnO	0.0312
BaO	0.038
Cr_2O_3	0.0486
ZrO_2	0.0649
P_2O_5	0.166
ClO	0.248
CaO	0.623
MgO	0.833
TiO_2	0.852
Na_2O	1.12
SO_3	2.73
Fe_2O_3	3.355
K_2O	3.98
CO_2	6.22
Al_2O_3	12.4
SiO_2	67.22

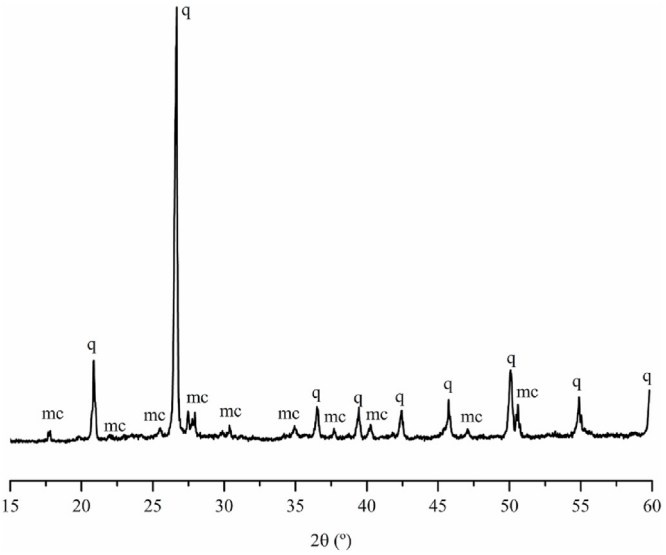

Fig. 2. X-ray diffraction pattern for the soil (mc - Muscovite, q - Quartz).

3.2. Definition of the mixture and specimen preparation

Considering the high-water content of the original soil, the mixing process followed the methodology recommended by Bruce et al. (2013) and Kitazume and Terashi (2013), where the volume of water required in the mixture was only provided by the original wet soil, to which all other components were added in powder form.

A previous study, developed by the authors (Pinheiro et al., 2019) using the response surface method to optimize the stabilisation of this soil and slag, has demonstrated that the stabilised soil can achieve a UCS of 0.73 MPa after 7 d, when cured in saltwater. It was based on that study that an activator solution was defined, combining sodium silicate (SS) and sodium hydroxide (SH), in a 1:1 proportion. The sodium hydroxide concentration varies between 6.5 and 8.5 mol/kg depending on the mixture.

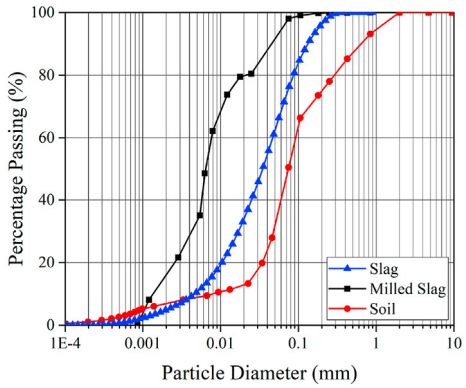

Fig. 3. Particle size distribution of the soil and slag before and after milling.

Table 3
Chemical composition of the slag (wt%).

SiO_2	Al_2O_3	CaO	MgO	MnO	Fe total	Cr_2O_3	Others
19.6	10.5	24.1	8.2	5.3	23.8	3.4	4.3

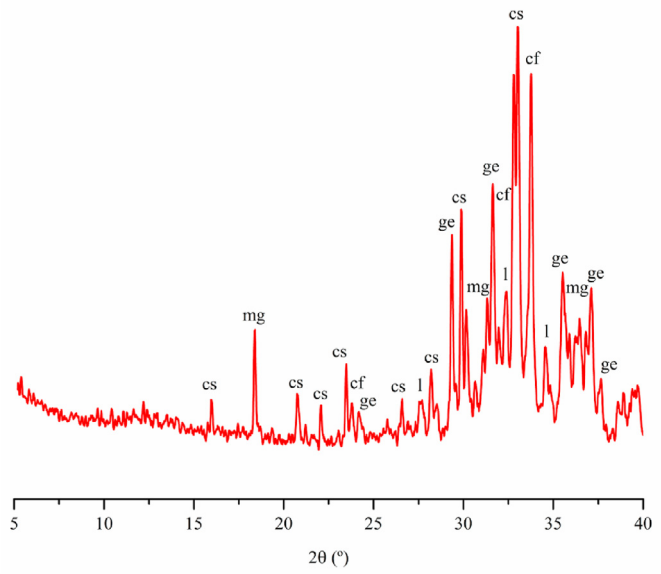

Fig. 4. X-ray diffraction pattern for the slag (SG) (cf - Calcium/magnesium/iron, cs - Calcium silicate, ge - Gehlenite, l - Larnite, mg - Magnetite).

As reported in the literature (Phummiphan et al., 2016; Sargent et al., 2016; Arulrajah et al., 2018), the precursor content is very influential on the strength development. These authors reported a precursor/soil ratio of 1:2.33 (using fly ash - FA), 1:13.5 (GGBFS), and 1:1.33 (slag and fly ash), respectively. For the present study, as presented in Table 4, a precursor/soil ratio of 1:1 was considered necessary, due to the unfavourable conditions for the alkaline activation found on site: the natural acidity of the contaminated soil; the underwater curing (which inevitably reduces the alkali concentration); and the low reactivity of the main precursor (i.e. the ladle slag), especially when compared with other types of slag reported in the literature (e.g. GGBFS). Moreover, in the case of the dry DSM, the fluidity of the binder is not important, as the AAC is injected in powder form, and since the ladle slag has not yet commercial value, its high amount will not increase the final cost.

The specimen preparation procedure started by mixing the precursor with the activator, and then the saturated soil was added resulting in a paste transferred to metal prismatic moulds of 4 cm × 4 cm × 16 cm. Both the mixing procedures and the mould dimensions followed European Committee for Standardization (2005). The specimens were demoulded after 24 h followed by 48 h of additional curing in a temperature-controlled room, at 20 °C, before being submerged in water.

To establish a threshold, additional specimens were fabricated with Portland cement type CEM I 52.5R. The binder content for these specimens was based on BS EN 14679 (2005) and Bruce (2000, 2001), which indicated that, for DSM in sands, 100–400 kg of cement should be used to treat 1 m^3 of soil. In this work, a precursor/soil ratio of 1:6.5 was selected, and this mixture was called Soil + CEM throughout the paper.

For the unconfined compression and flexural tests, elastic stiffness evaluation and leaching analysis, the curing water was sea water (pH value = 7.34) at 20 °C. For the triaxial compression tests, the specimens were submerged in distilled water (pH value = 5.4) at 20 °C, which is more acid than the saltwater, and for that reason the sodium hydroxide concentration was increased from 6.5 mol/kg to 8.5 mol/kg.

Table 4 shows the characteristics of the mixtures. Note that the liquid/solids (L/S) was higher in the control group (Soil + CEM) than in the Soil + SG mixtures, because the water in the mixture is originated only from the saturated soil. Since the Soil + CEM has a higher proportion of soil than Soil + SG, it has also a higher water content. Additionally, it is also indicated the tests performed on each mixture, as described in the following sections: flexural and unconfined compressive strength tests (UCS), evaluation of maximum shear modulus (G_0) through seismic wave velocities, leaching tests, and triaxial tests.

3.3. Flexural and compressive strengths

To evaluate the mechanical performance of the different mixtures, after different curing periods, flexural and compressive strength tests were performed and analysed according to EN 196-1 (2005). Several authors (Terashi, 1997, 2003; Bruce, 2000, 2001; Kitazume et al., 2015; Yan et al., 2019) used unconfined compression strength tests to evaluate the mechanical performance of DSM improved soils. However, Larsson et al. (2012) showed that bending should be considered as an important failure mode in the design of DSM columns, thus justifying the flexural strength tests in the present study.

The flexural strength was evaluated with 3-points load tests, with the flexural strength F_s calculated by (EN 196-1, 2005):

$$F_s = 1.5F_f l / b^3 \quad (1)$$

where F_s is the flexural strength (MPa), b is the side of the square section of the prism (mm), F_f is the load applied to the centre of the prism at failure (N), and l is the distance between the supports (mm).

The compression test was performed on both halves of the failed prism. The result of the flexural strength test was calculated as the arithmetic mean of three individual results, while the result of the compressive strength was calculated as the arithmetic mean of the resulting six individual halves.

3.4. Seismic wave measurements

Seismic P- and S-wave propagation time through the specimens was also measured, using ultrasonic transducers. From the

Table 4
Composition of the studied mixtures.

Mixture name	Tests performed	Soil/precursor	L/S	Precursor/activator	SS/SH	SH molal concentration	Curing water
Soil + SG_mix1	UCS, G_0 and leaching	1	0.28	2.5	1	6.5	Sea water
Soil + CEM	UCS, and G_0	6.5	0.26	–	–	–	Sea water
Soil + SG_mix2	Triaxial tests	1	0.14	2.5	1	8.5	Distilled water

elasticity theory, it is known that the shear wave velocities are related to the maximum shear modulus (G_0), according to Eq. (2), and the Poisson's ratio can be derived by the combination of the two velocities according to Eq. (3) The readings were taken in curing periods of 3 d, 7 d, 14 d and 28 d, considering the first direct arrival of the output wave method (Viana da Fonseca et al., 2009), where the direct measurement of the time interval between the input and output waves assumes the plane wavefronts and the absence of any reflected or refracted waves. The description of the experimental setup, calibration and measuring procedure is fully described in Rios et al. (2017).

$$G_0 = \rho V_S^2 \tag{2}$$

$$\nu = \frac{\left(\frac{V_P}{V_S}\right)^2 - 2}{2\left(\frac{V_P}{V_S}\right)^2 - 2} \tag{3}$$

where V_P is the velocity of the P wave (m/s), V_S is the velocity of the S wave (m/s), and ρ is the bulk density of the material (g/cm^3).

3.5. Leachate testing

The chemical analysis of the leachate recovered from purposely fabricated specimens aims to assess the possible release of heavy metals from the contaminated soil or the steel slag. The leachate tests on the stabilised soil were carried out according to the procedure described in the BS EN 12457 (2002) standard. The tests were performed after 3-, 7-, 14- and 28-d curing. The 3-d curing was chosen to assess the environmental behaviour at younger ages, when there is a greater risk of the heavy metals in the soil-binder combination to be released into the surrounding water (since the binder is still at an early development age). The 28-d coincides with the longer curing period also used for the mechanical testing, a time when it is expected that lower heavy metals molecules are released. The concentrations obtained from the eluate were compared with the limits defined in the LER 1701 (2004).

3.6. Triaxial compression tests

Two sets of specimens were submitted to triaxial tests: one set was cured without any confining stress, while the other was cured in a triaxial cell, with a pre-determined confining stress. Both groups were sheared in monotonic triaxial compression, under three distinct confining pressures, after three curing periods of 7 d, 14 d and 28 d, which resulted in a total of $2 \times 3 \times 3 = 18$ tests.

Three days after moulding, to ensure enough strength to avoid disintegration in water, the group cured under stress was placed on the triaxial cell with the corresponding confining pressure, and then the specimens were sheared at 7 d, 14 d or 28 d. Cemented soils are difficult to saturate and the saturation degree is not easily or reliably evaluated (Rios et al., 2014). For this reason, there was no attempt to saturate the specimens using high back-pressures. Instead, these were soaked in water (with relatively low back-pressures of 10 kPa) aiming only to minimize the suction effect on final strength.

To provide similar conditions to both groups except on the curing stress, the group cured without stress was submerged in distilled water, 3 d after moulding. The specimens were kept submerged until being installed in the triaxial cell, after 7 d, 14 d or 28 d. The shearing occurred in the same day, after application of the corresponding confining stress.

Effective isotropic confining stresses of 35 kPa, 50 kPa and 150 kPa were selected to reproduce the effective horizontal stresses acting on a DSM column at depths of 9 m, 12 m and 37 m, considering a unit weight of 18 kN/m^3 for the stabilised soil and a coefficient of earth pressure at rest of 0.5. For research purposes, to quantify the stress-curing effect on an upper boundary, to understand if and how a higher curing stress could influence its behaviour. Fig. 5 illustrates some of the steps used on the triaxial tests.

4. Results and discussion

4.1. Flexural and compressive strengths

The results regarding the evolution of the flexural and compressive strength tests after 3-, 7-, 14- and 28-d curing, are

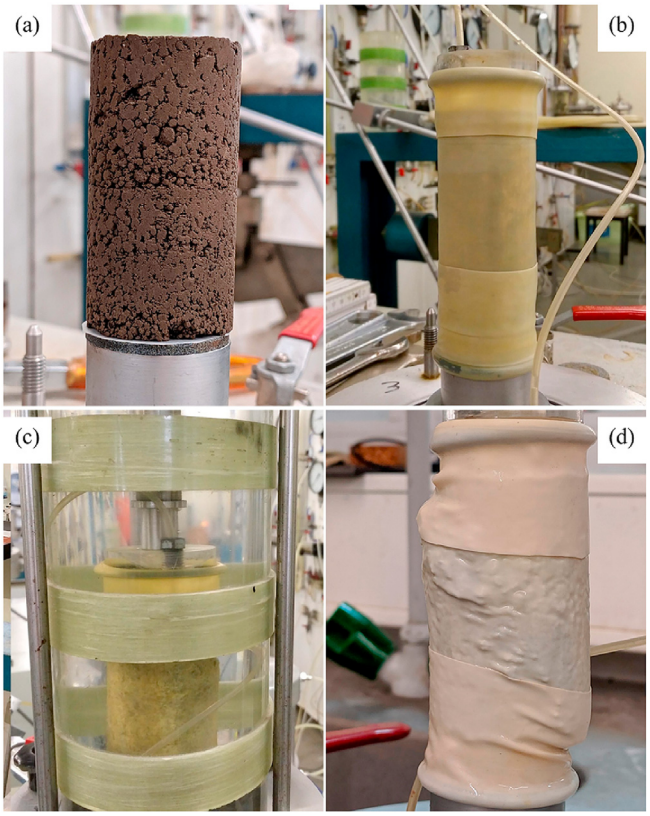

Fig. 5. Triaxial test phases for Soil + SG_mix2 as described in Table 4: (a) General view of the installation of the specimen in the triaxial cell, (b) Application of the membrane, (c) Mounting of the Perspex cell, and (d) Specimen after shearing.

shown in Fig. 6. Both flexural and compressive strength rates are significantly higher in Soil + SG_mix1 in comparison with the Soil + CEM mixture. Although the SG-based mixture showed initial (3 d) lower flexural strength values than the CEM-based mixture, after 28 d the flexural strength of the SG-based mixture is already 65% higher than the CEM-based mixture. Conversely to other studies (Arulrajah et al., 2018) where the Soil + CEM presented higher flexural strength than the soil stabilised with the AAC for all curing periods (up to 28 d), in this work the flexural strength of the Soil + SG_mix1 was higher than that of the Portland cement-based mixture already at 14 d. Regarding the UCS, the relative performance was even more favourable to the Soil + SG_mix1 mixtures, which showed more than twice the UCS of the Soil + CEM mixture, regardless of the curing period considered. This indicates that the ratio between flexural strength and UCS is much higher for the Soil + CEM mixture, in agreement with the results of Arulrajah et al. (2018) which attributed this difference to the flocculated structure of the AAC for high binder contents. This structure was also observed in Fig. 5a and the impact of this type of cementation on other properties such as elastic stiffness is presented further below.

The experimental points showed in Fig. 6 were adjusted by a mathematical expression developed for Portland cement-based binders (Cristelo et al., 2015). The ACI (1997) recommends Eq. (4) to estimate the compressive strength at a given curing day, $(f'_c)_t$, based on the reference value at 28-d, $(f'_c)_{28}$, where a and β are the experimental coefficients that should be between 0.05 and 9.25, and between 0.67 and 0.98. For specimens of Portland cement CEM class 52.5 N with moist curing the ACI (1997) suggests that $a = 2.3$ and $\beta = 0.92$, which adjust quite well to the Soil + CEM flexural and compressive strength results. However, for the Soil + SG_mix1, new values were needed and different parameters were obtained for compressive and flexural strengths. These values summarised in Table 5 are outside the prescribed ranges as a different behaviour was observed in the Soil + SG_mix1 as mentioned above.

$$(f'_c)_t = \frac{t}{a+\beta t}(f'_c)_{28} \quad (4)$$

Despite the acidity of the soil, the submerged curing, and the low reactivity of the precursor, these strength values are higher than those obtained in other similar studies, most likely due to the significant slag content. Other authors, like Sargent et al. (2016), obtained UCS values, after 28 d, of approximately 2.1 MPa, while Arulrajah et al. (2018) reported UCS values between 6 MPa and 7.5 MPa, in a stabilised clay, after 28 d. The UCS values for Soil + CEM are in the range of 0.5–5 MPa proposed by Terashi (2003) for stabilised granular soils at 28-d.

Table 5
Values of the constants a and β for each case.

Material	Test	Coefficients	
		a	β
Soil + SG_mix1	Compressive strength	3.14	0.91
	Flexural strength	12.34	0.57
Soil + CEM	Compressive strength	2.3	0.92
	Flexural strength	2.3	0.92

4.2. Elastic stiffness evolution with time

Compression (P) and shear (S) wave's propagation velocities were used to estimate the evolution, over the curing time, of the maximum shear modulus and Poisson's ratio of the tested mixtures. Fig. 7 shows the output signals obtained for the P and S waves, indicating the obtained propagation time recorded for each case, using a classic time domain approach (Viana da Fonseca et al., 2009). Each result shown in the figure corresponds to an average of several consecutive pulse measurements.

From Fig. 7, it is possible to observe the evolution of the propagation time throughout the curing period. The reduction of the S wave propagation time implies an increase of the propagation velocity, which consequently translates an increase in stiffness, according to Eq. (5). In addition, this increase in the S wave velocity is also followed by an increase in the P wave velocity as observed for other mixtures (Rios et al., 2017).

According to G_0 development presented in Fig. 8a, the Soil + SG_mix1 mixture showed a faster stiffness evolution than the Soil + CEM mixture, which started with a higher initial stiffness at young ages. This high rate of stiffness increase was also obtained by Rios et al. (2017) in a silty sand stabilised with an alkali-activated fly ash. The combination of P and S waves led to the evaluation of the Poisson's ratio (by Eq. (3)) for both mixtures as presented in Fig. 8b. The values measured for Soil + SG_mix1 start with 0.28 and reaching 0.2 at 28 d when the cementing structure is already developed. This is expected as the increase in cementation due to curing period prevents the soil structure to deform laterally when loaded in the vertical direction. For this reason, the ratio between horizontal and vertical strains (corresponding to the definition of Poisson's ratio) decreases. Rios et al. (2017) obtained similar values

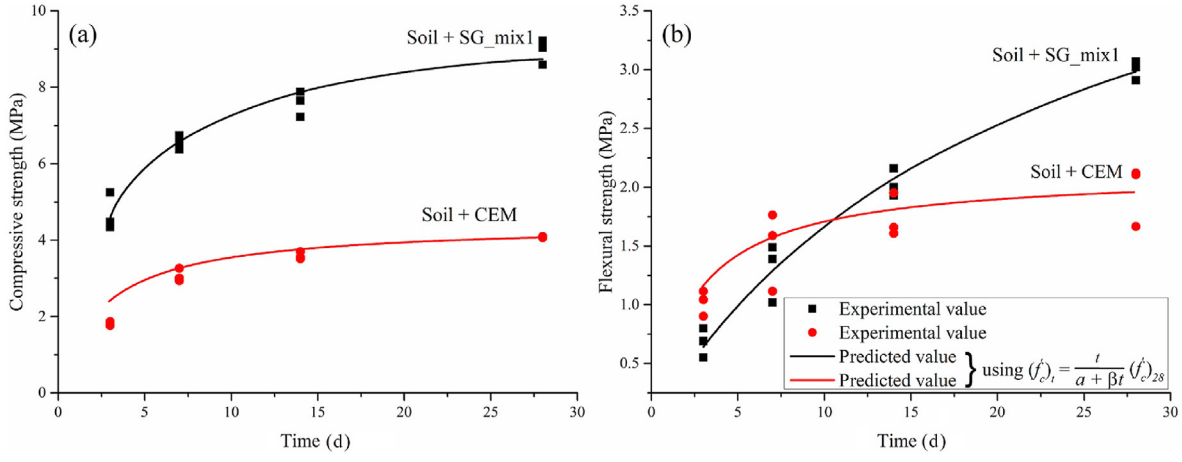

Fig. 6. Exponential models for flexural and compressive strengths, for both Soil + SG_mix1 and Soil + CEM mixtures, up to 28 d.

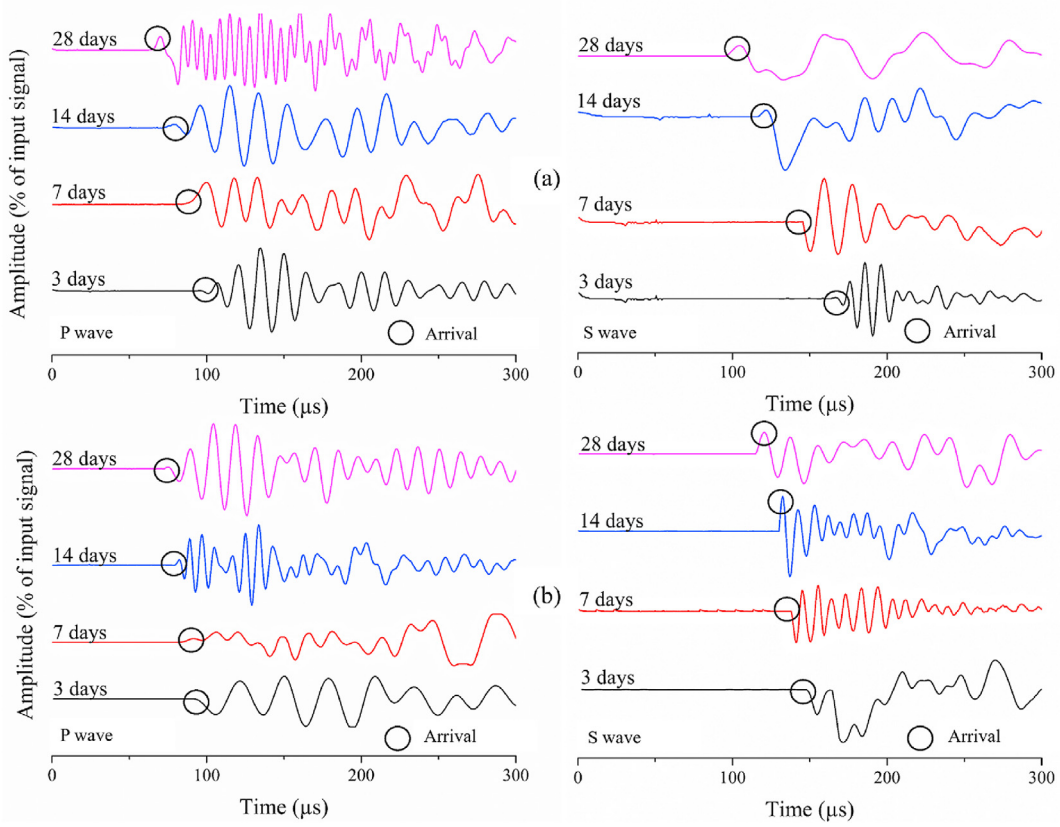

Fig. 7. Seismic wave propagation time for (a) Soil + SG_mix1 and (b) Soil + CEM.

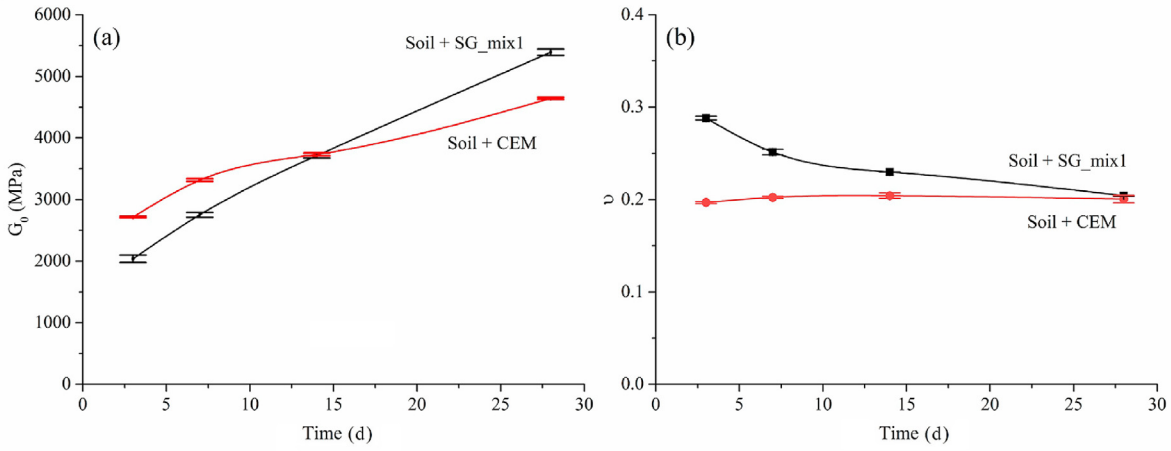

Fig. 8. Evolution of (a) the initial shear moduli (G_0) and (b) Poisson's ratio (υ) with curing time for the two materials.

between 28 d and 1 year of curing. The Soil + CEM has an almost constant Poisson's ratio value as a result of a smaller stiffness increase, with values around 0.2 for all ages, which agrees with the results obtained by (Narayan Swamy, 1971).

4.3. Correlation between strength and stiffness or flexural strength

In this work, the ratio G_0/UCS was analyzed throughout time, as presented in Fig. 9a, and non-linear equations (Eqs. (5) and (6)) were adjusted obtaining a correlation coefficient of $R^2 = 0.99$ for both materials. It is interesting to notice that after an initial decrease due to hardening of cementitious bonds, the G_0/UCS ratio has a slight increase, indicating that time has more effect on stiffness rather than strength. On the other hand, these results clearly express that the difference between Soil + SG_mix1 and Soil + CEM is much higher in strength than that in stiffness.

The flexural/compressive strength ratio, F_S/UCS, (Fig. 9b) increases with time for the Soil + SG_mix1 and decreases with time for the Soil + CEM, both mixtures achieving closer values at 28 d. This indicates that in the short term, the Soil + SG_mix1 mixtures

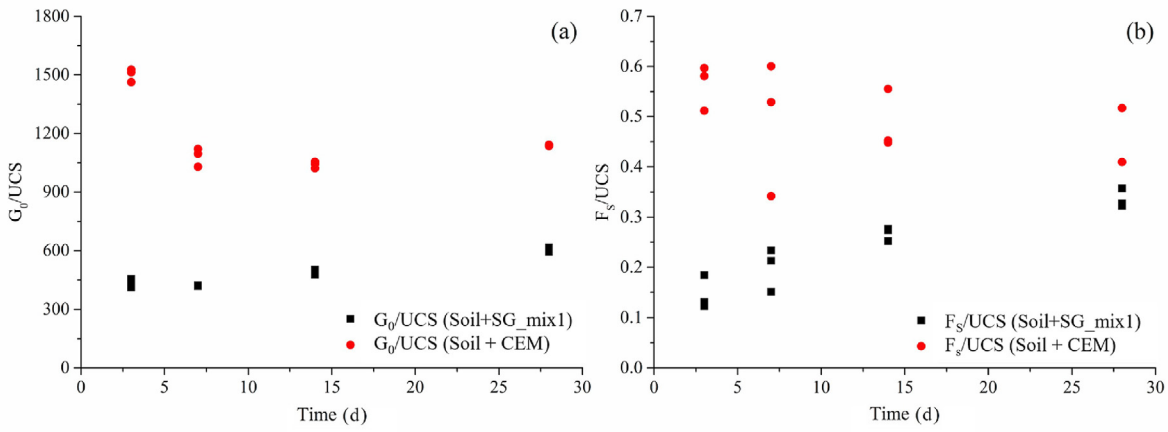

Fig. 9. Relationship between G_0/UCS (a) and F_S/UCS (b) and its evolution in time.

have a much higher increase in compressive strength than that in flexural strength conversely to what occurs in the Soil + CEM mixtures.

Despite the higher scatter of flexural strength results, this agrees well with the evolution of the G_0/UCS ratio presented in Fig. 9a. Based on these results, it seems that the flocculated structure of the Soil + SG_mix1 discussed before has an impact on the elastic stiffness and flexural strength of the material. These properties do not show the same enhanced performance (of the Soil + SG_mix1 in comparison to Soil + CEM) as it was observed for UCS.

$$\left(\frac{G_0}{UCS}\right)_{SG} = 788.07 + \frac{-6366.11}{t} + \frac{34476.9}{t^2} + \frac{-55692.4}{t^3} \quad (5)$$

$$\left(\frac{G_0}{UCS}\right)_{CEM} = 1345.4 + \frac{-7552.16}{t} + \frac{51687.7}{t^2} + \frac{-82913.5}{t^3} \quad (6)$$

where G_0 is the shear modulus (MPa), UCS is the compressive strength (MPa), and t is the time (d).

4.4. Leachate analysis

Fig. 10 shows the environmental performance of the original (for comparison purposes) and stabilised soil, after four different curing periods. Based on the information collected from Alam et al. (2019) and on the composition of the original soil (Table 2), the chemical analysis of the recovered leachate solutions focused on Arsenic (As), Chromium (Cr), Copper (Cu), Lead (Pb), Zinc (Zn), Chlorides (Cl^-) and Sulphates (SO_4^{2-}), as these elements have already been identified, also, in the work conducted by Santos-Ferreira et al. (2015). For these elements, the obtained concentrations are presented together with the limit values indicated in European Union (LER 1701, 2004) for inert wastes limits.

All concentrations measured on the treated specimens were below the limits defined by the European Union (LER 1701, 2004) for waste acceptable as 'inert'. Even elements that are usually difficult to immobilize, like Arsenic (Keimowitz et al., 2002; Zhang and Itoh, 2005) and Copper (Ahmari and Zhang, 2013) are below the threshold values. It should be noted that, even if the original soil leaching values are below the limits, these elements frequently leach from the slag (included in the 4.3% found in Table 3 and named as "Others") in the presence of an alkaline medium (Ahmari and Zhang, 2013; Fernandez-Jimenez et al., 2005) and could thus represent a threat. However, the application of the AAC proved to be an effective stabiliser of those contaminants.

The analysis of Fig. 10 also showed high concentrations of chloride, from the seawater, and sulphate, from the seawater and the soil. Usually, that contaminants attack the concrete made with common Portland cement (Al-Amoudi et al., 1992; Ke et al., 2017). It is common the use of special types of cement to improve the chemical resistance against adverse environments (for example, saline conditions). However, in this case, the stabilised soil + binder combination was able to maintain its structural and environmental integrity.

Based on this leaching analysis, the proposed stabilisation was able to effectively immobilize the contaminants making the material adequate for the DSM treatment.

4.5. Effect of curing under stress

Fig. 11 shows the stress-strain curves obtained in the triaxial tests performed in Soil + SG_mix2 (Table 4), representing the variation of the deviatoric stress (q) and volumetric strain (ε_V) with the axial strain (ε_a). Unfortunately, these tests could not be performed with local instrumentation due to constraints related with the use of AAC. For this reason, the volumetric strains presented in Fig. 11 are a gross external measurement made by the water that flows in and out the cell.

Brittle stress-strain curves, typical of strong bonded soils (Rios et al., 2014), were observed, showing a well-defined peak stress followed by strain softening. The mentioned peak stress increased with curing time. It is also clear that specimens submitted to higher confining pressures showed a higher peak stress, indicating that the confining pressures were not able to destroy the cementation bonds.

In terms of volumetric behaviour at younger ages (Fig. 11b), the specimens showed an initial contraction, followed by a significant dilation. The development of cementation during curing increased the dilatant behaviour. As expressed by other authors (Viana da Fonseca, 1996, 1998; Schnaid et al., 2001), in strong bonded soils, the maximum rate of dilation does not generally coincides with the peak stress as observed in uncemented soils, occurring slightly after the peak stress, indicating that the peak is influenced by the cementation level.

The behaviour of the specimens was similar, irrespectively of the curing stress, for stress-strain curves at the same confining stress and curing age. This is an important finding, indicating that, for the studied curing periods, the material can be evaluated in the laboratory without curing stress, and the results can be representative of the material behaviour in a DSM column, where it will cure

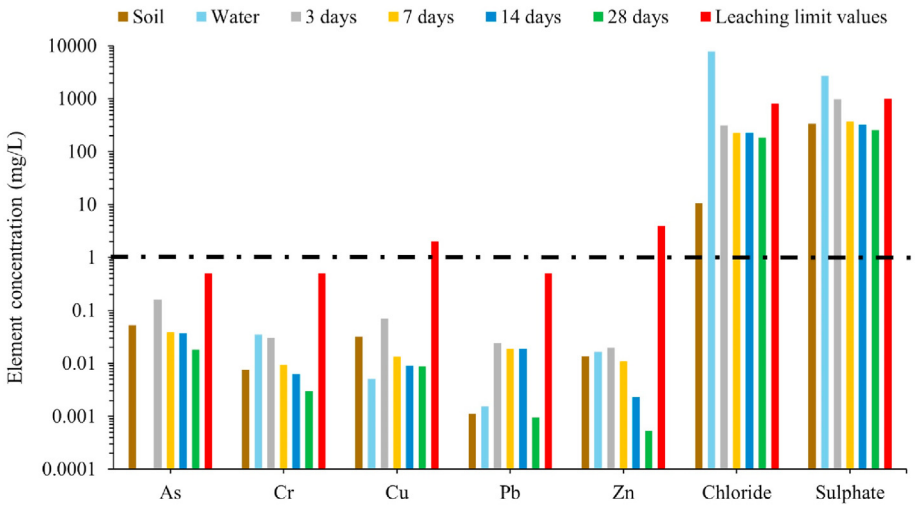

Fig. 10. Element concentrations in the leaching solution obtained from soil, sea water and the mixtures in 4 different ages and comparison with the acceptance limits defined in 2003/33/EC for inert wastes limits. The dashed-dot black line represents a concentration of 1. Because the scale of the graph is logarithmic, this helps in the interpretation.

under the weight of the column. This behaviour is a consequence of the early age strength of this material, which, after 7 d curing, already possesses enough strength to support moderate confining stresses without bond breakage. Since these materials tend to develop for a long time (Cristelo et al., 2011; Phetchuay et al., 2016), this study needs to be enlarged for higher curing periods. However, from the obtained results, which have already addressed the most important part of the cementing structure development, it is not expected that curing stress may have a significant impact.

The ultimate strength failure's envelopes for both curing conditions are shown in Fig. 12, for each applied confining stress. Since a shear plane failure was obtained, as observed in Fig. 5d, a procedure based on the analysis of Mohr's circles used by Gasparre (2005) was applied to calculate the stresses acting on the rupture plane. For this purpose, the angle of the shear plane failure was necessary, where a 55° was measured as observed in Fig. 5d. In each case, the results were adjusted by linear regression and the parameter φ'_{cv} obtained. In all the cases, the points present a very good alignment enabling high coefficients of correlation ($R^2 = 0.99$). Although the tests did not have enough instrumentation to distinguish between the cement contribution and the dilatant contribution, a reasonable estimate of φ'_{cv} was possible since this is an intrinsic property of the soil, independent of the initial compactness state of the specimen and related to friction. The friction angle at constant volume (φ'_{cv}) varied between 45° and 49° in the improved soil specimens, which is within the values obtained for cemented soils by other authors (Schnaid et al., 2001; Rios et al., 2014).

Since the curing stress effect is minor, Table 6 summarises the strength parameters obtained for the three curing periods, by doing the average of the results obtained with or without stress. In Table 6, there is also the ratio between the deviatoric stress at peak and in ultimate conditions (q_{peak}/q_{cv}), an indicator of the material brittleness which, as expected, increases with curing time. The secant stiffness modulus at 50% of peak strength (E_{50}) obtained in the stress-strain curves was added to the table which also demonstrates the increase in stiffness due to curing. From these E_{50} values, the stiffness evolution with effective stress was derived using the well-established Janbu (1963) relationship:

$$E_{50} = k_{50} P_a \left(\frac{\sigma'_3}{P_a}\right)^{n_{50}} \quad (7)$$

where P_a is the atmospheric pressure considered to be 100 kPa; and k_{50} and n_{50} are the parameters obtained from the triaxial tests for each curing time, as indicated in Table 6.

It is interesting to notice that n_{50} values remain approximately constant, as a sign that the stiffness evolution with depth has a similar trend for all the curing periods. However, the k_{50} values increase with curing time as a result of the enhanced stiffness due to cementation.

5. Conclusions

The present work describes the treatment of a costal/estuarine contaminated sediment with a binder made by the alkaline activation of a ladle slag. Although less reactive this ladle slag with no commercial value was previously milled to increase its reactivity and subsequently activated with sodium hydroxide and sodium silicate. To achieve an optimum mixture capable of complying with the harsh conditions existing at the site, a high amount of alkali-activated ladle slag was used to stabilise the soil.

The mechanical behaviour of this mixture was analysed and compared with a reference soil-cement mixture. When tested in unconfined compression, the specimens treated with the alkali-activated slag showed better mechanical resistance than the mixture with Portland cement for all curing periods. However, when analysing the flexural strength or the maximum shear modulus obtained from the seismic wave's measurements, the specimens with Portland cement show higher initial strength and stiffness but, during time it is overpassed by the specimen treated with alkali-activated slag. The stiffness/strength ratio indicates that the difference between both mixtures is higher in strength than in stiffness which can be attributed to the flocculated nature of AAC structure.

The evolution of the Poisson's ratio with time showed that Soil + CEM mixture presented an approximately constant value with time as a result of a smaller stiffness increase, while the values measured for Soil + SG_mix1 start with 0.28 reaching 0.2 at 28 d when the cementing structure is already developed. This is expected as the increase in cementation due to curing period, prevents the soil structure to deform laterally reducing the obtained Poisson ratio.

In terms of environmental performance, the specimen treated with alkali-activated slag presented a very satisfactory

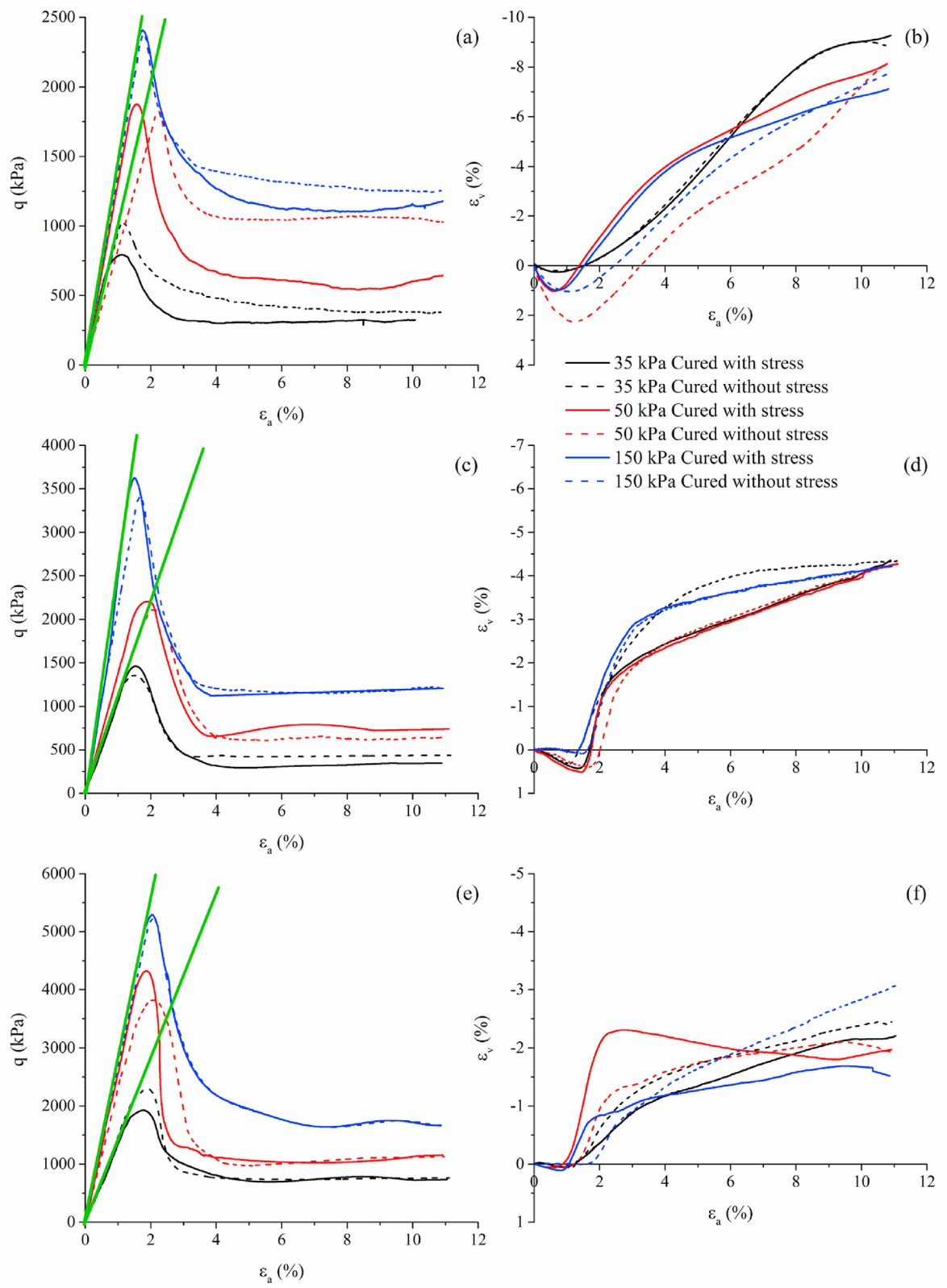

Fig. 11. Stress-axial strain-volumetric strain curves for specimens improved with AAC: (a, b) 7 d; (c, d) 14 d; and (e, f) 28 d.

performance, not exceeding the values included in European environmental legislation for waste inert materials (the Council Decision 2003/33/EC (LER 1701, 2004)) in any of the evaluated ages.

Triaxial compression tests performed with and without curing stress indicated that this effect does not seem to be very significant in this material because of its early age strength. After 7 d of curing,

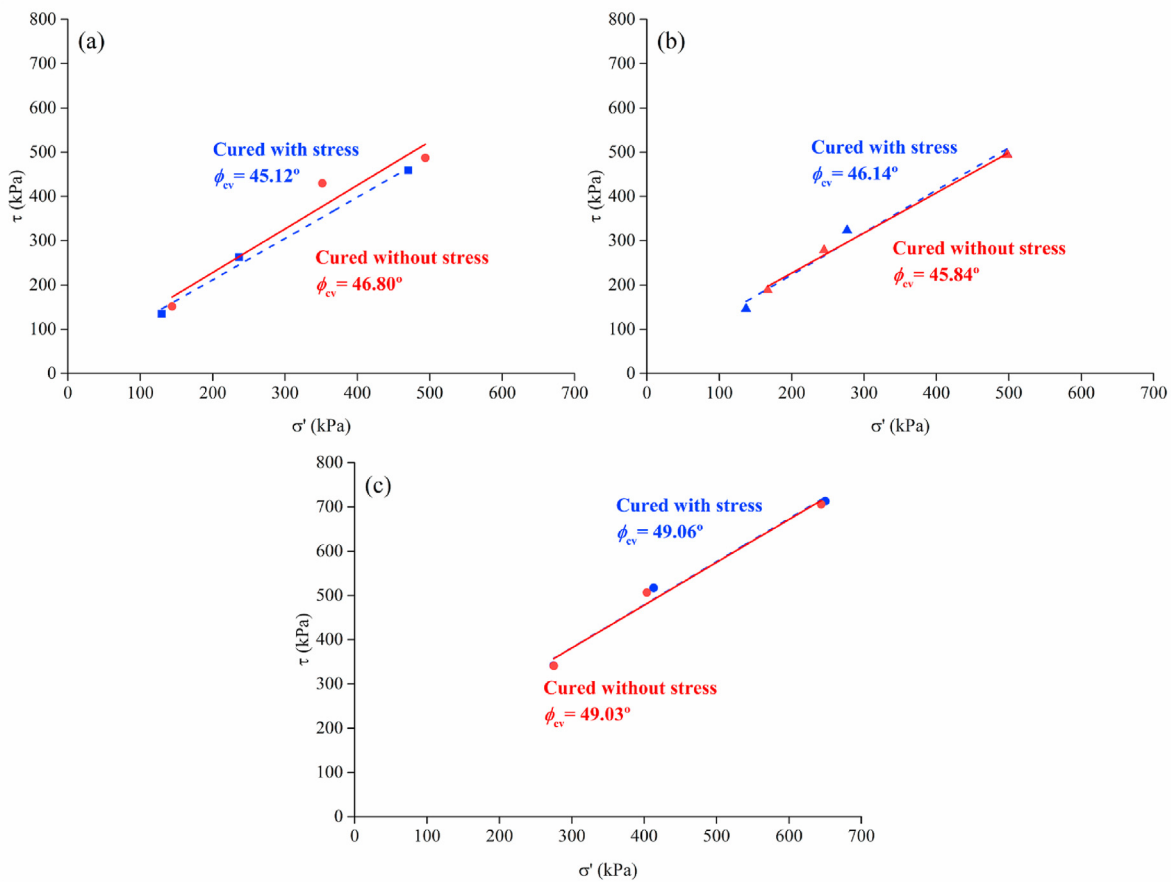

Fig. 12. Ultimate strength envelopes for (a) 7 d, (b) 14 d, and (c) 28 d with and without stress during curing.

Table 6
Strength and stiffness parameters derived from triaxial compression tests.

Curing time (d)	p'_0 (kPa)	k_{50}	n_{50}	E_{50} (MPa)	q_{peak}/q_{cv}	φ'_{cv} (°)
7	35	1208.04	0.5	70.32	2.58	45.96
	50			107.26	2.26	
	150			141.02	2.01	
14	35	1790.52	0.5	106.93	3.61	45.99
	50			124.94	2.93	
	150			222.46	2.9	
28	35	2491.74	0.4	137.5	2.89	49.05
	50			243.81	3.7	
	150			277.97	3.27	

the material already possesses enough strength to support moderate confining stresses without bond breakage. These tests also enabled the evaluation of high values of friction angles (between 45° and 50°) and secant modulus at 50% of peak strength (between 70 kPa and 300 kPa) both increasing with curing time.

This analysis suggests that an alkali-activated binder derived from a ladle slag without market value may be an effective alternative to Portland cement for stabilising contaminated sediments below the water table. However, the environmental and economic implications associated with the more extensive use of slag and the resulting demand for different processes, such as grinding and activation, need to be considered in future studies.

Declaration of competing interest

The authors declare that they have no known competing financial interests or personal relationships that could have appeared to influence the work reported in this paper.

Acknowledgments

This work received funding from CNPq (Brazilian council for scientific and technological development) through 201465/2015-9 scholarship of the “Science without borders” program. The second author acknowledges the support of MCTES/FCT (Portuguese Science and Technology Foundation of Portuguese Ministry of Science and Technology) through CEECIND/04583/2017 grant. This work was also financially supported by: Base Funding - UIDB/04708/2020 of the CONSTRUCT - Instituto de I&D em Estruturas e Construções - funded by national funds through FCT/MCTES (PIDDAC). A special acknowledgment is also due to the Portuguese National Steel Industry of Maia, part of MEGASA group, for the steel slag supply and to Professor Joaquim Faria for his support in understanding the basic notions of chemistry.

References

Adesanya, E., Ohenoja, K., Kinnunen, P., Illikainen, M., 2017. Properties and durability of alkali-activated ladle slag. Mater. Struct. 50, 255.

Ahmari, S., Zhang, L., 2013. Durability and leaching behavior of mine tailings-based geopolymer bricks. Construct. Build. Mater. 44, 743–750.
Alam, Q., Schollbach, K., van Hoek, C., van der Laan, S., de Wolf, T., Brouwers, H.J.H., 2019. In-depth mineralogical quantification of MSWI bottom ash phases and their association with potentially toxic elements. Waste Manag. 87, 1–12.
Al-Amoudi, O.S.B., Abduljauwad, S.N., Maslehuddin, M., 1992. Effect of chloride and sulfate contamination in soils on corrosion of steel and concrete. Transport. Res. Rec. 7, 1992.
ACI, 1997. Prediction of Creep, Shrinkage and Temperature Effects in Concrete Structures. American Concrete Institute (ACI) Committee 209 Report.
Arulrajah, A., Yaghoubi, M., Disfani, M.M., Horpibulsuk, S., Bo, M.W., Leong, M., 2018. Evaluation of fly ash- and slag-based geopolymers for the improvement of a soft marine clay by deep soil mixing. Soils Found. 58, 1358–1370.
ASTM D2487-11, 2011. Standard Practice for Classification of Soils for Engineering Purposes (Unified Soil Classification System). ASTM International, West Conshohocken, Pennsylvania.
BS EN 14679, 2005. Execution of Special Geotechnical Works - Deep Mixing. British Standards Institution.
BS EN 12457, 2002. Characterisation of Waste. Leaching. Compliance Test for Leaching of Granular Waste Materials and Sludges. British Standards Institution.
Bruce, C., Collin, J., Berg, R., Filz, G., Terashi, M., Yang, D., 2013. Federal highway administration design manual: deep mixing for embankment and foundation support. FHWA-HRT-13-046. Offices of Research & Development, Federal Highway Administation, United States.
Bruce, D.A., 2001. Practitioner's guide to the deep mixing method. Proc. Inst. Civ. Eng.-Ground Improv. 5, 95–100.
Bouassida, M., Fattah, M.Y., Mezni, N., 2022. Bearing capacity of foundation on soil reinforced by deep mixing columns. Geomechanics Geoengin 17, 309–320.
Bruce, D.A., 2000. An Introduction to the Deep Soil Mixing Methods as Used in Geotechnical Applications. FHWA-RD-99-138. Offices of Research & Development, Federal Highway Administation, United States.
Cortes-Garcia, L.D., Chartier, M., 2022. 2D and 3D numerical modeling of a cellular deep soil mix earth retention structure. In: Geo-Congress 2022. American Society of Civil Engineers, pp. 325–334.
Cristelo, N., Glendinning, S., Teixeira Pinto, A., 2011. Deep soft soil improvement by alkaline activation. Proc. Inst. Civ. Eng.-Ground Improv. 164, 73–82.
Cristelo, N., Miranda, T., Oliveira, D.V., et al., 2015. Assessing the production of jet mix columns using alkali activated waste based on mechanical and financial performance and CO_2 (eq) emissions. J. Clean. Prod. 102, 447–460.
EN 196-1, 2005. Methods of Testing Cement - Part 1: Determination of Strength. European Committee for Standardization.
Fernandez-Jimenez, A., Palomo, A., Macphee, D.E., Lachowski, E.E., 2005. Fixing arsenic in alkali-activated cementitious matrices. J. Am. Ceram. Soc. 88, 1122–1126.
Freitag, P., Maurer, H., Reichenauer, T.G., 2021. Selection of optimized binders for dechlorination of trichloroethylene-contaminated sites by jet grouting and deep soil mixing. J. Environ. Eng. 147 (11). https://doi.org/10.1061/(ASCE)EE.1943-7870.0001926.
Gao, X., Yuan, B., Yu, Q.L., Brouwers, H.J.H., 2017. Characterization and application of municipal solid waste incineration (MSWI) bottom ash and waste granite powder in alkali activated slag. J. Clean. Prod. 164, 410–419.
Gasparre, A., 2005. Advanced Laboratory Characterization of London Clay. PhD Thesis. Imperial College London, London, UK.
Grant Norton, M., Provis, J.L., 2020. 1000 at 1000: geopolymer technology—the current state of the art. J. Mater. Sci. 55, 13487–13489.
Gupta, S., Kumar, S., 2023. A state-of-the-art review of the deep soil mixing technique for ground improvement. Innov. Infrastruct. Solut. 8, 129.
Hasheminezhad, A., Bahadori, H., 2019. Seismic response of shallow foundations over liquefiable soils improved by deep soil mixing columns. Comput. Geotech. 110, 251–273.
ISO 14688-2, 2017. Geotechnical Investigation and Testing - Identification and Classification of Soil - Part 2: Principles for a Classification. International Organization for Standardization.
ISO 17892-3, 2015. Geotechnical Investigation and Testing - Laboratory Testing of Soil - Part 3: Determination of Particle Density. International Organization for Standardization.
ISO 17892-4, 2016. Geotechnical Investigation and Testing - Laboratory Testing of Soil - Part 4: Determination of Particle Size Distribution. International Organization for Standardization.
ISO 17892-12, 2018. Geotechnical Investigation and Testing - Laboratory Testing of Soil - Part 12: Determination of Liquid and Plastic Limits. International Organization for Standardization.
Jamsawang, P., Voottipruex, P., Boathong, P., Mairaing, W., Horpibulsuk, S., 2015. Three-dimensional numerical investigation on lateral movement and factor of safety of slopes stabilized with deep cement mixing column rows. Eng. Geol. 188, 159–167.
Janbu, N., 1963. Soil compressibility as determined by oedometer and triaxial tests. In: Proceedings of the European Conference on Soil Mechanics and Foundation Engineering, pp. 245–251.
Ke, X., Bernal, S.A., Provis, J.L., 2017. Uptake of chloride and carbonate by Mg-Al and Ca-Al layered double hydroxides in simulated pore solutions of alkali-activated slag cement. Cement Concr. Res. 100, 1–13.
Keimowitz, A.R., Simpson, H.J., Stute, M., et al., 2002. Naturally occurring arsenic: mobilization at a landfill in Maine and implications for remediation. Appl. Geochem. 20, 1985–2002.
Kitazume, M., Grisolia, M., Leder, E., et al., 2015. Applicability of molding procedures in laboratory mix tests for quality control and assurance of the deep mixing method. Soils Found. 55, 761–777.
Kitazume, M., Terashi, M., 2013. The Deep Mixing Method. CRC Press.
Larsson, S., Malm, R., Charbit, B., Ansell, A., 2012. Finite element modelling of laterally loaded lime–cement columns using a damage plasticity model. Comput. Geotech. 44, 48–57.
LER 1701, 2004. Council Decision 2003/33/EC of 19 December 2002. Official Journal of the European Union.
Maher, A., Douglas, W.S., Yang, D., Jafari, F., Schaefer, V.R., 2007. Cement deep soil mixing (CDSM) for solidification of soft estuarine sediments. Mar. Georesour. Geotechnol. 25, 221–235.
Mohammadinia, A., Disfani, M.M., Conomy, D., Arulrajah, A., Horpibulsuk, S., Darmawan, S., 2019. Utilization of alkali-activated fly ash for construction of deep mixed columns in loose sands. J. Mater. Civ. Eng. 31, 04019233.
Mohammed, M.A., Mohd Yunus, N.Z., Hezmi, M.A., Abang Hasbollah, D.Z., Rashid, A.S., 2021. Ground improvement and its role in carbon dioxide reduction: a review. Environ. Sci. Pollut. Res. 28, 8968–8988.
Narayan Swamy, R., 1971. Dynamic Poisson's ratio of Portland cement paste, mortar and concrete. Cement Concr. Res. 1, 559–583.
Nguyen, T.V., Rayamajhi, D., Boulanger, R.W., et al., 2013. Design of DSM grids for liquefaction remediation. J. Geotech. Geoenviron. Eng. 139, 1923–1933.
Phair, J.W., van Deventer, J.S.J., Smith, J.D., 2004. Effect of Al source and alkali activation on Pb and Cu immobilisation in fly-ash based "geopolymers.". Appl. Geochem. 19, 423–434.
Phetchuay, C., Horpibulsuk, S., Arulrajah, A., Suksiripattanapong, C., Udomchai, A., 2016. Strength development in soft marine clay stabilized by fly ash and calcium carbide residue based geopolymer. Appl. Clay Sci. 127–128, 134–142.
Phummiphan, I., Horpibulsuk, S., Sukmak, P., Chinkulkijniwat, A., Arulrajah, A., Shen, S.-L., 2016. Stabilisation of marginal lateritic soil using high calcium fly ash-based geopolymer. Road Mater. Pavement Des. 17, 877–891.
Pinheiro, C., Rios, S., Viana da Fonseca, A., 2021. Comparative assessment of soil behavior by in situ and laboratory tests. In: Proceedings of the 6th International Conference on Geotechnical and Geophysical Site Characterization.
Pinheiro, C., Rios, S., Viana da Fonseca, A., Coelho, J., Fernández-Jiménez, A., Cristelo, N., 2019. Soil stabilized with alkali activated slag at various concentrations of activator. In: Wastes: Solutions, Treatments and Opportunities. CRC Press, pp. 451–456.
Pinheiro, C., Rios, S., Viana da Fonseca, A., Fernández-Jiménez, A., Cristelo, N., 2020. Application of the response surface method to optimize alkali activated cements based on low-reactivity ladle furnace slag. Construct. Build. Mater. 264, 120271.
Provis, J.L., 2018. Alkali-activated materials. Cement Concr. Res. 114, 40–48.
Provis, J.L., van Deventer, J., 2014. Alkali Activated Materials, vol. 13. first ed. Springer, Dordrecht, Netherlands.
Rakhimova, N., 2022. Recent advances in alternative cementitious materials for nuclear waste immobilization: a review. Sustainability 15, 689.
Rios, S., Cristelo, N., Viana da Fonseca, A., Ferreira, C., da Fonseca, A.V., Ferreira, C., 2017. Stiffness behavior of soil stabilized with alkali-activated fly ash from small to large strains. Int. J. GeoMech. 17, 04016087.
Rios, S., da Fonseca, A.V., Cristelo, N., Pinheiro, C., 2018. Geotechnical properties of sediments by in situ tests. In: Sustainable Civil Infrastructures. Springer, Cham, pp. 59–68.
Rios, S., Viana da Fonseca, A., Baudet, B.A., 2014. On the shearing behaviour of an artificially cemented soil. Acta Geotech. 9, 215–226.
Robertson, P.K., 2009. Interpretation of cone penetration tests - a unified approach. Can. Geotech. J. 46, 1337–1355.
Santos-Ferreira, A., Dias, E., Da Silva, P.F., Santos, C., Cabral, M., 2015. Dredging of Vila do Conde harbor, Portugal - contamination of sediments. Procedia Eng. 116, 939–946.
Sargent, P., Hughes, P.N., Rouainia, M., 2016. A new low carbon cementitious binder for stabilising weak ground conditions through deep soil mixing. Soils Found. 56, 1021–1034.
Schnaid, F., Prietto, P.D.M., Consoli, N.C., 2001. Characterization of cemented sand in triaxial compression. J. Geotech. Geoenviron. Eng. 127, 857–868.
Shao, Y., Macari, E.J., Cai, W., 2005. Compound deep soil mixing columns for retaining structures in excavations. J. Geotech. Geoenviron. Eng. 131, 1370–1377.
Sukmak, P., De Silva, P., Horpibulsuk, S., Chindaprasirt, P., 2015. Sulfate resistance of clay-Portland cement and clay high-calcium fly ash geopolymer. J. Mater. Civ. Eng. 27, 04014158.
Talha Junaid, M., Kayali, O., Khennane, A., 2017. Response of alkali activated low calcium fly-ash based geopolymer concrete under compressive load at elevated temperatures. Mater. Struct. 50, 50.

Terashi, M., 2003. The state of practice in deep mixing methods. In: Grouting and Ground Treatment. American Society of Civil Engineers, Reston, VA, 2003.
Terashi, M., 1997. Theme lecture: deep mixing method-Brief state of the art. In: Proceedings of the 14th ICSMFE, 4, pp. 2475–2478.
Turner, L.K., Collins, F.G., 2013. Carbon dioxide equivalent (CO_2-e) emissions: a comparison between geopolymer and OPC cement concrete. Construct. Build. Mater. 43, 125–130.
Tyagi, S., Annachhatre, A.P., 2023. A review on recent trends in solidification and stabilization techniques for heavy metal immobilization. J. Mater. Cycles Waste Manag. 25, 733–757.
Venda Oliveira, P.J., Pinheiro, J.L.P., Correia, A.A.S., 2011. Numerical analysis of an embankment built on soft soil reinforced with deep mixing columns: parametric study. Comput. Geotech. 38, 566–576.
Viana da Fonseca, A., 1998. Identifying the reserve of strength and stiffness characteristics due to cemented structure of a saprolitic soil from granite. The geotechnics of hard soils-soft rocks. In: Proceedings of the 2nd International Symposium on Hard Soils-Soft Rocks, pp. 361–372. Naples.
Viana da Fonseca, A., Ferreira, C., Fahey, M., 2009. A framework interpreting bender element tests, combining time-domain and frequency-domain methods. Geotech. Test J. 32, 91–107.
Viana da Fonseca, A., 1996. Geomecânica dos Solos Residuais do Granito do Porto: Critérios para dimensionamento de fundações directas. PhD Thesis. FEUP - Faculdade de Engenharia da Universidade do Porto (in Portuguese).
Wang, F., Wang, H., Al-Tabbaa, A., 2015. Time-dependent performance of soil mix technology stabilized/solidified contaminated site soils. J. Hazard Mater. 286, 503–508.
Yan, B., Kouame, K.J.A., Tannant, D., Lv, W., Cai, M., 2019. Effect of fly ash on the mechanical properties of cemented backfill made with brine. Geotech. Geol. Eng. 37, 691–705.
Zhang, F.-S., Itoh, H., 2005. Iron oxide-loaded slag for arsenic removal from aqueous system. Chemosphere 60, 319–325.
Zuo, J., Wang, B., Li, W., Han, S., Wang, J., Zhang, F., 2023. Quality assessment and quality control of deep soil mixing columns based on a cement-content controlled method. Sci. Rep. 13, 4813.

Sara Rios is Assistant Research Fellow in the Geotechnical group of the Department of Civil Engineering of the Faculty of Engineering of the University of Porto. She obtained her MSc degree in Soil Mechanics and Geotechnical Engineering from University of Coimbra in 2008 and the PhD in Civil Engineering from University of Porto in 2011 studying the geomechanical behaviour of an artificially cemented silty sand. From 2013 to 2018, she has concluded a Post-doc on alkali activated binders. Sara Rios has also participated in several national and European research projects as well as in industry consultancy services, and she gives lectures in the Civil Engineering Master Course of FEUP. She is a member of TC307 – Sustainability in Geotechnical Engineering from the International Society of Soil Mechanics and Geotechnical Engineering (ISSMGE). She is Associate Editor of *Soils and Rocks* and *Journal of Materials in Civil Engineering* from ASCE. Her main research interests are: (i) static and cyclic characterisation of natural and artificial soils; (ii) ground improvement technologies including the use of Portland cement, alkali activated binders made from industrial by-products (such as slag or fly ash), or rubber from end of life tires; (iii) constitutive modelling; (iv) numerical analysis of earth structures; and (v) sustainability in Geotechnical Engineering.